Correction of the Secondary Voltage of Coupling Capacitor Voltage Transformers in Real Time

C. A. Silva, D. Fernandes Jr., *Member, IEEE*, and W. L. A. Neves, *Member, IEEE*

Abstract -- In this paper, a compensator device capable of performing the correction of the CCVT model secondary voltage in real time, is presented. The methodology is based on a technique for recursive digital filtering of the CCVT secondary voltage. The parameters of the compensator are obtained from the transfer function of the CCVT model and from the ideal frequency response of the compensated CCVT. To evaluate the compensation technique two case studies are analyzed: harmonic distortion at the 230 kV system and a phase to ground fault at the 230 kV system. Real time simulations attest that the compensator acts to bring the secondary voltage waveform close to the primary voltage signal. This may be important for the correct indication of measuring devices and proper operation of protection systems.

Index Terms--CCVT model, digital signal processing, electromagnetic transients, real time simulations.

I. INTRODUCTION

UTILITIES that work with geration and transmission of electrical power utilize the coupling capacitor voltage transformer (CCVT) for measurement and protection in High Voltage (HV) and Extra High Voltage (EHV) systems. The protection of electrical power system is primarily controlled by relays. Therefore, the proper functioning of the system is limited by the accuracy action of the relays, which in turn, are subject to errors inherent to the instrument transformers, such as current transformer (CT), step down transformer (SDT) and the coupling capacitor voltage transformers.

The CCVTs inability to reproduce the primary voltage waveform at its secondary terminal may cause some problems for distance relays. During a fault on the transmission line, the voltage collapses at the CCVT primary side and the energy stored in capacitors and inductors may produce voltage swings that have significant amplitude and duration that affect the performance of protective relays [1].

In this context, this work presents a device capable of performing the correction of the secondary voltage of a

C. A. Silva is Ph.D. student of Electrical Engineering at Federal University of Campina Grande (UFCG), Av Aprígio Veloso, 882, Bodocongó, 58429-140, Campina Grande-PB, (e-mail: celio.silva@ee.ufcg.edu.br).

D. Fernandes Jr. and W. L. A. Neves are with Department of Electrical Engineering of UFCG, (e-mails: damasio@dee.ufcg.edu.br, waneves@dee.ufcg.edu.br).

CCVT. The device is basically a recursive digital filter whose parameters are obtained from the CCVT frequency response assuming a predefined topology. The evaluation of the device is performed through real time simulations with the device connected to the RTDS$^{\text{TM}}$ (Real Time Digital Simulator).

The analysis of dynamic compensation for a 230 kV CCVT from Companhia Hidro Elétrica do São Francisco (CHESF) is presented. To evaluate the compensation strategy two case studies were performed: measurement of harmonic distortion in 230 kV systems and fault studies. Computer simulations carried out in real time prove that the dynamic compensation of the CCVT secondary voltage may enhance the performance and reliability of the protection system.

II. COUPLING CAPACITOR VOLTAGE TRANSFORMER

A basic circuit diagram for a typical CCVT at 60 Hz is shown in Fig. 1.
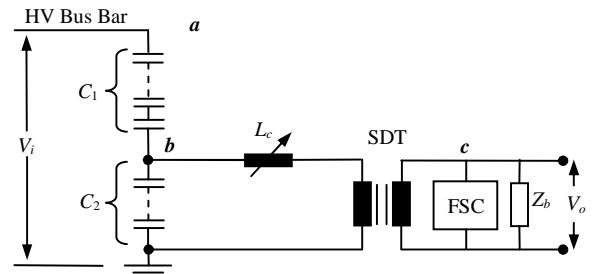

Fig. 1. Electrical basic diagram for a typical CCVT.

The CCVT primary consists of two capacitive elements connected in series (C_1 and C_2), with an intermediate derivation **b** which corresponds to a voltage typically between 10 kV and 20 kV, which feeds the primary winding of a step down transformer (SDT), which provide a secondary voltage V_o to the measurement and protection instruments. The compensating inductor (L_c) is designed to control the voltage lag in the capacitive divider.

Under certain conditions, for example, an unsuccessful reclosing of a transmission line, or after clearing of short-circuit in the CCVT secondary, ferroresonance may take place. This phenomenon is basically the resonance of the circuit capacitance with the iron core nonlinear inductance. In order to damp out ferroresonance oscillations, a ferroresonance suppression circuit (FSC) has been used across the SDT winding. It should be pointed out that the type of

ferroresonance filter in the CCVT plays an important role in the response of the CCVT.

The diagram shown in Fig. 1 is valid only near power frequency. A model to be applicable for frequencies up to a few kilohertz needs to take into account the SDT primary winding and the compensating inductor stray capacitances [3]-[5].

III. DESIGN OF THE COMPENSATOR

The correction of the CCVT secondary voltage will be performed by using a recursive digital filter, here denominated by compensator. According to the literature, techniques for correction of CCVT secondary voltage to be programmable in DSP (Digital Signal Processor) are based on the inverse of the CCVT transfer function. However, studies are limited due to the use of a simplified CCVT model and the absence of a methodology for obtaining the model parameters.

Here, the CCVT model reported in [3] is used and shown in Fig. 2. It takes into account the SDT primary winding, the compensating inductor stray capacitances, and a passive ferroresonance filter. This model is fairly accurate for a frequency range from 10 Hz to 10 kHz.
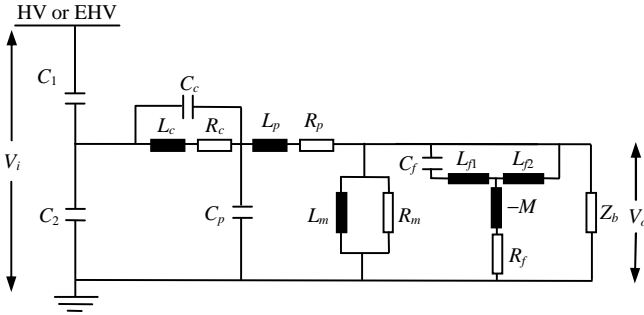

Fig. 2. CCVT model used for linear parameters estimation [3].

The design of the compensator takes basically five steps:

1. Frequency response measurements;

2. Computation of the CCVT model parameters;

3. Computation of the recursive digital filter coefficients;

4. Implementation of the recursive digital filter;

5. Validation of the technique through real time simulations.

A. Frequency Response Measurements

In order to obtain the frequency response data to be used as input data to the routine developed to compute the CCVT parameters, frequency response measurements, for magnitude and phase, were carried out for a 230 kV CCVT, in a frequency range from 10 Hz to 10 kHz [6], shown in Fig. 3 and 4.
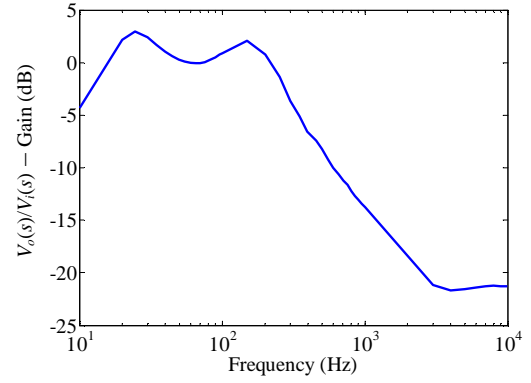

Fig. 3. Magnitude curve of the 230 kV CCVT voltage ratio [6].
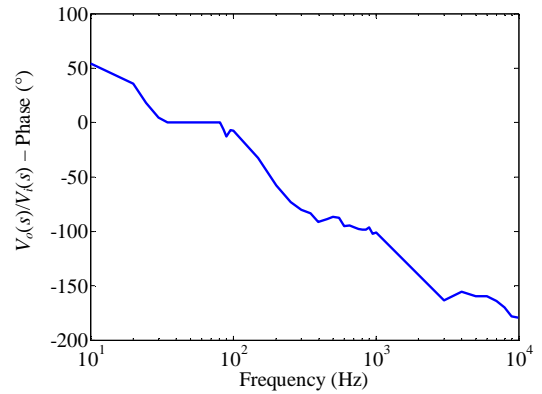

Fig. 4. Phase curve of the 230 kV CCVT voltage ratio.

B. Computation of the CCVT Model Parameters

The CCVT parameters were obtained from frequency response data points of magnitude and phase measured curves. A software (TPCalc), developed by the authors [7], was used to compute the parameters. The software computes the parameters of the model of Fig. 2 to fit the transfer functions represented by the ratio V_o/V_i. It is an iterative procedure based on Newton's method. The estimated parameters are shown in Table I.

TABLE I
ESTIMATED PARAMETERS FOR THE 230 kV CCVT AFTER THE
FITTING PROCEDURE

$C_1 = 5.65$ nF	$C_p = 16.1$ pF	$L_{f1} = 4.58$ mH
$C_2 = 81.1$ nF	$R_p = 625.7\ \Omega$	$C_f = 220.2\ \mu$F
$R_c = 2.91$ kΩ	$L_p = 96.9$ H	$L_{f2} = 32.78$ mH
$L_c = 1.61$ H	$R_m = 579.3$ MΩ	$R_f = 4.33\ \Omega$
$C_c = 31.5$ nF	$L_m = 129.1$ kH	$M = 4.34$ mH

The magnitude and phase curves for the measured (red color) and fitted (blue color) voltage ratios are shown in Fig. 5 and Fig. 6, respectively.
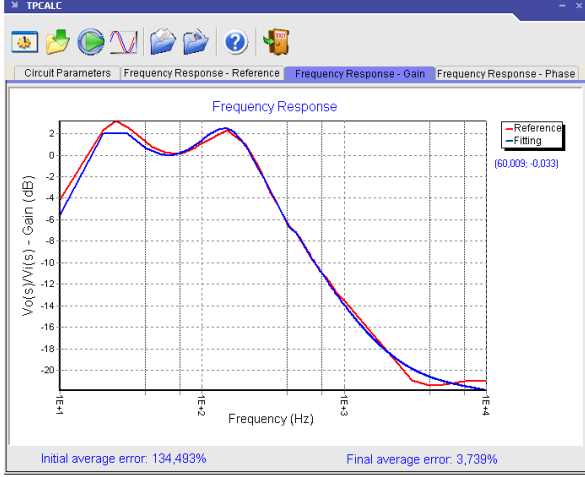
Fig. 5. 230 kV CCVT frequency response magnitude: measured (red curve); fitted (blue curve).
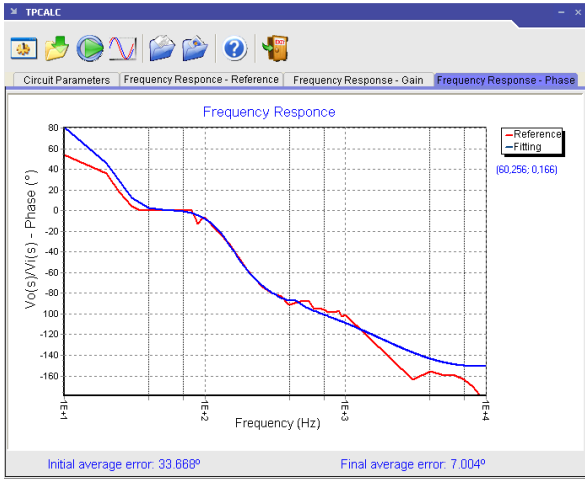

Fig. 6. 230 kV CCVT frequency response phase: measured (red curve), set (blue curve).

As shown at the bottom of the Figs. 5 and 6, the initial error, before starting the iterative procedure, for the magnitude and phase were 134.493% and 33.668°, respectively. After the fitting procedure, the errors computed with the fitting parameters were 3.739% for the magnitude and 7.004° for the phase.

C. Computation of Recursive Digital Filter Coefficients

According to [6], the CCVT voltage ratio for the model shown in Fig. 4 can be expressed as:

$$G_{TPC}(s) = \frac{V_0(s)}{V_i(s)} = \frac{A_7 s^7 + A_6 s^6 + A_5 s^5 + A_4 s^4 + A_3 s^3 + A_2 s^2}{B_8 s^8 + B_7 s^7 + B_6 s^6 + B_5 s^5 + B_4 s^4 + B_3 s^3 + B_2 s^2 + B_1 s + B_0} . \quad (1)$$

The coefficients A_n, $n = 2, ..., 7$ e B_m, $m = 0, ..., 8$ in (1) are nonlinear functions of the elements R, L and C of the CCVT model. Note that (1) is a special case of rational function presented in (2) with two zeros at the origin, where, z_n, $n = 1, ..., 7$ e p_m, $m = 1, ..., 8$ are the zeros and poles, respectively, of the rational function approximate.

$$H_{CCVT}(s) = \frac{(s+z_1)(s+z_2)(s+z_3)(s+z_4)(s+z_5)(s+z_6)(s+z_7)}{(s+p_1)(s+p_2)(s+p_3)(s+p_4)(s+p_5)(s+p_6)(s+p_7)(s+p_8)} . \quad (2)$$

Representing the frequency response by a rational function in the form of poles and zeros, it is possible to avoid instability problems during the implementation of high-order filter.

For an ideal compensation, i.e., unity gain for the frequency range of interest and a minimum phase shift between the primary and secondary voltage, the transfer functions of the compensator and the CCVT should present the following relation:

$$H_{CCVT}(s).G_{Comp}(s) = 1 . \quad (3)$$

According to (3), the transfer function of compensator, $G_{comp}(s)$, is obtained by the direct inversion of the CCVT transfer function, $H_{CCVT}(s)$. However, the inversion of $H_{CCVT}(s)$ would produce an unstable compensator, since the transfer function of compensator would have the number of zeros greater than the number of poles. Besides, it would have double poles at the origin. Here, as a solution of the mentioned inconveniences, (3) is modified to:

$$H_{CCVT}(s).G_{Comp}(s).\varphi(s) = 1 , \quad (4)$$

where, $\varphi(s)$ is an improper rational function (the number of poles is greater than the number of zeros). Thus, the transfer function of compensator takes the form of (5),

$$G_{Comp}(s) = [H_{CCVT}(s).\varphi(s)]^{-1} . \quad (5)$$

Replacing (5) in (3):

$$\varphi(s)^{-1} = 1 . \quad (6)$$

The rational function $\varphi(s)^{-1}$ will impose the dynamic behavior of the compensated CCVT.

In order to cancel the undesirable poles in the inversion of $H_{CCVT}(s)$, $\varphi(s)^{-1}$ should have at least a double zero at the origin. This characteristic of $\varphi(s)^{-1}$ can be considered its first boundary condition. As a second condition, it is desirable that when $\omega \to 0$, $\varphi(s)^{-1} \to 0$, i.e., $\varphi(s)^{-1}$ should have at least two zeros (at the origin) and three poles. Taking into account these two conditions, the simplest expression for the transfer function of the compensated CCVT is given by:

$$\varphi(s)^{-1} = \frac{s^2}{D_3 s^3 + D_2 s^2 + D_1 s + D_0} . \quad (7)$$

Since $\varphi(s)^{-1}$ is a nonlinear function in the coefficients D_3, D_2, D_1 and D_0, they were estimated from a nonlinear least squares technique, the Levenberg-Marquardt method. After the adjustment procedure, the coefficients shown in (8) were obtained. The magnitude and phase curves of the transfer function for the compensated CCVT are shown in Figs. 7 and 8, respectively.

Note that the magnitude and phase of $\varphi(s)^{-1}$ have acceptable behavior, i.e., unity gain and very small phase shift in the range from 10 Hz to 10 kHz.
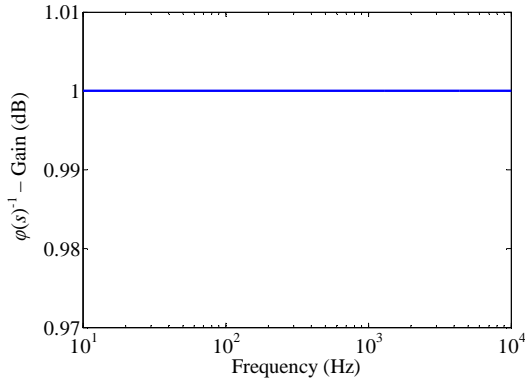
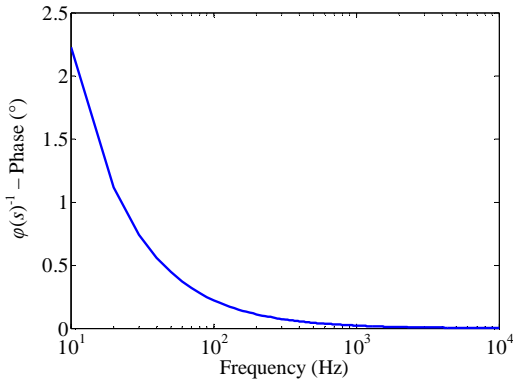Fig. 7. Magnitude of the transfer function for the compensated CCVT.

Fig. 8. Phase of the transfer function for the compensated CCVT.

$$\varphi(s)^{-1} = \frac{s^2}{4.85 \times 10^{-10} \times s^3 + 1.00 \times s^2 + 2.44 \times s + 2.98}. \qquad (8)$$

D. Implementation of the Recursive Digital Filter

High order filters when directly performed become highly sensitive to the computation of their coefficients, since any change in one coefficient of numerator or denominator may modify the dynamic behavior of the filter [8]. To overcome this problem, a method to dispose the connection of sub-filters with second-order in cascade is presented here in an algorithm:

1. Decompose the transfer function of the analog filter in the form of poles and zeros;
2. Determine the poles, or pair of poles near the origin;
3. Determine the zero, or pair of zeros near the pole, or pair of poles, found in step 2;
4. Combine these poles and zeros in filters of second order sections;
5. Repeat steps 2-4 until all the poles and zeros have been combined into second-order sections;
6. The final disposition of the cascades should obey the order of increasing or decreasing distance of the poles from the origin of the s plane.

Using this algorithm, the transfer function of compensator, $G_{Comp}(z)$ in z domain, may be written in the form of second order sub-filters connected in cascade, as expressed in (10),

$$G_{Comp}(z) = \frac{V_{0\,Comp}(z)}{V_0(z)} = k_0 \prod_{i=1}^{4} \frac{k_{i1} + k_{i2}z^{-1} + k_{i3}z^{-2}}{1 + k_{i4}z^{-1} + k_{i5}z^{-2}}, \qquad (10)$$

where, k_0 and k_{ij}, with $i = 1, ..., 4$ and $j = 1, ..., 5$ are the escaling constant of the filter and the coefficients of second order recursive digital filter, respectively. The escaling constant of the filter is the ratio between a value of secondary voltage v_0 and the compensated secondary voltage v_{0Comp} in an operating point n, and the coefficients k_{ij} are obtained from the bilinear transformation applied to the second order sub-filters in s domain.

E. Validation of the Technique Through Real Time Simulations

The RTDS^{TM} uses essencially the same methods used in EMTP (Electromagnetic Transients Program) type programs, with the simulation time step of 50 µs.

The validation of the methodology was performed in two stages: in the first one, the CCVT and compensator was used to monitor voltage signals with harmonic components, and in the second stage, the behavior of the compensated CCVT was evaluated for fault occurrence. All simulations to validate the efficiency of the method were implemented in the RTDS^{TM} (Real Time Digital Simulator). In all analyzed cases, the results obtained with the presence of the compensator were compared to the reference voltage, i.e., the CCVT primary voltage.

For validation purposes, a fictitious electric system consisting of three sources of harmonics and two transmission lines, shown in Fig. 9, was used.
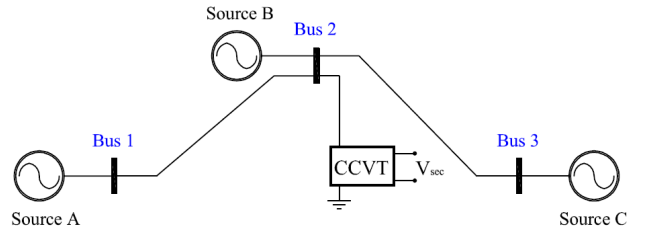

Fig. 9. Electrical system used for measurement of harmonics in 230 kV transmission systems.

Transmission lines were represented using the Bergeron's method [9]. The data of transmission lines (200 km long) were obtained from an actual line belonging to the 230 kV electrical system of CHESF (Companhia Hidro Elétrica do São Francisco), the Norteast Brazilian utility. The values of resistance, reactance and susceptance zero and positive sequence are shown in Table II.

TABLE II
TRANSMISSION LINE DATA

Sequence	R (Ω/km)	X (Ω/km)	ωC (µΩ^{-1}/km)
Zero	0.4309	1.5659	2.3301
Positive	0.0888	0.5249	3.1210

The voltage sources at phase a for buses 1, 2 and 3, in kV, are respectivelly:

$$v_{A(Bus1)} = \frac{230.\sqrt{2}}{\sqrt{3}}.\sin(\omega t) + \frac{230.\sqrt{2}}{3.\sqrt{3}}.\sin(3.\omega t) + \frac{230.\sqrt{2}}{5.\sqrt{3}}.\sin(5.\omega t) +$$
$$+ \frac{230.\sqrt{2}}{7.\sqrt{3}}.\sin(7.\omega t) + \frac{230.\sqrt{2}}{9.\sqrt{3}}.\sin(9.\omega t)$$

$$v_{A(Bus2)} = \frac{230.\sqrt{2}}{\sqrt{3}}.\sin(\omega t - 5°) + \frac{230.\sqrt{2}}{11.\sqrt{3}}.\sin(11.\omega t) + \frac{230.\sqrt{2}}{13.\sqrt{3}}.\sin(13.\omega t) +$$
$$+ \frac{230.\sqrt{2}}{15.\sqrt{3}}.\sin(15.\omega t) + \frac{230.\sqrt{2}}{17.\sqrt{3}}.\sin(17.\omega t)$$

$$v_{A(Bus3)} = \frac{230.\sqrt{2}}{\sqrt{3}}.\sin(\omega t - 10°) + \frac{230.\sqrt{2}}{19.\sqrt{3}}.\sin(19.\omega t) + \frac{230.\sqrt{2}}{21.\sqrt{3}}.\sin(21.\omega t) +$$
$$+ \frac{230.\sqrt{2}}{23.\sqrt{3}}.\sin(23.\omega t) + \frac{230.\sqrt{2}}{25.\sqrt{3}}.\sin(25.\omega t)$$

For phases *b* and *c*, the RTDS^{TM} computes magnitude and phase angles for the voltage sources automatically [9]. In fact the magnitude of each harmonic component at each bus is the same as its corresponding harmonic source at phase *a*, but their phase angles changes depending on their harmonic sequence. For instance, in phase *b* and *c* positive sequence harmonics introduces a -120° and +120° shift, respectively, whereas negative sequence harmonics introduces a +120° and -120° shift, respectively.

In order to evaluate the compensator behavior under a phase to ground fault at the CCVT primary side, the system shown in Fig. 10 was used.
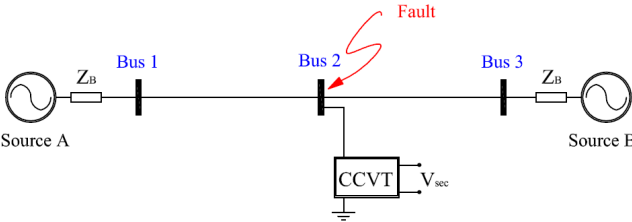

Fig. 10. Electrical system used for evaluation of the CCVT secondary voltage compensator in protection system.

The electrical system consists of two voltages sources with their respective impedances and transmission lines (200 km long), whose data are the same shown in Table II. The data system are presented in Table III.

TABLE III
DATA OF THE 230 kV EQUIVALENTE SYSTEM

Source	Voltage (kV)	R_0 (Ω)	X_0 (Ω)	R_1 (Ω)	X_1 (Ω)
A	187.8/0°	0.2856	5.5610	2.0205	7.2720
B	187.8/-10°	0.8644	12.2484	12.8150	31.7268

IV. RESULTS

A. The Compensator for Measurement Applications

With the real time implementation of the electrical system shown in Fig. 9, several simulations were performed. Fig. 11 shows the CCVT primary and secondary voltage waveforms during the measurement of harmonic distortion without the presence of the compensator (recursive digital filter), both expressed in p.u.

Based on the curves shown in Fig. 11, one can observe that the secondary voltage (without compensation) does not

reproduce correctly some frequency components. Therefore, measurements of signals with harmonic distortion may present significant errors when the CCVT is not compensated.
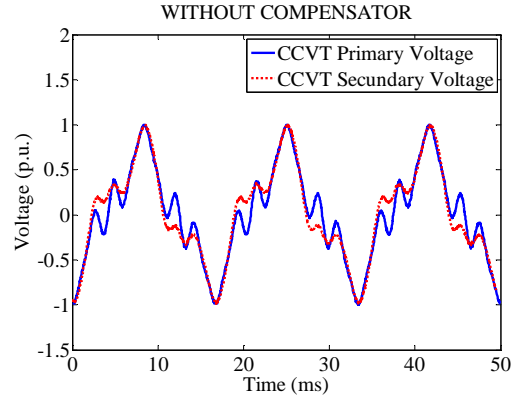

Fig. 11. Operation of the CCVT without the compensator: measurement of harmonic distortion.

The performance of the CCVT with compensator for measurement of harmonic distortion in power systems is shown in Fig. 12. It is observed that the compensator proposed in this work is an alternative to enable the CCVT to be used for measurements of harmonics with good accuracy.
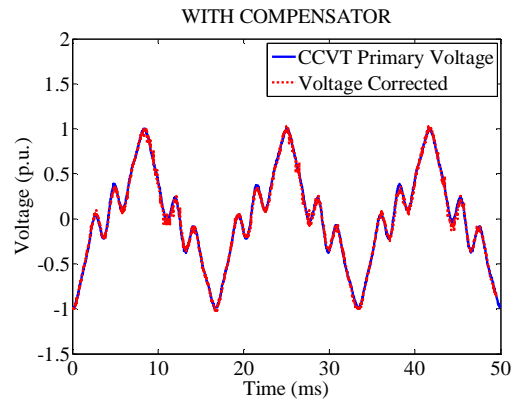

Fig. 12. Operation of the CCVT with the compensator: measurement of harmonic distortion.

In the next section is presented the compensator behavior for protection applications.

B. The Compensator for Protection Applications

The effectiveness of the compensator to correct the secondary voltage of the CCVT for a phase to ground fault is addressed comparing the waveforms, obtained for the situation in which the compensator is ignored (Fig. 13) to the waveforms obtained for the situation in which the compensator is taken into account (Fig. 14). One can see that the compensator is a good alternative to correct the CCVT secondary voltage during a fault.

It can be seen in Fig. 12 and 14 that the compensator device introduces quite noticeable noise. That is because, at this stage, the compensator device is assembled in a protoboard, which is very sensitive to the external environment and to grounding. Compensator devices used in connection with

digital relays in service would have internally a set of filters to eliminate noise coming from the external environment.
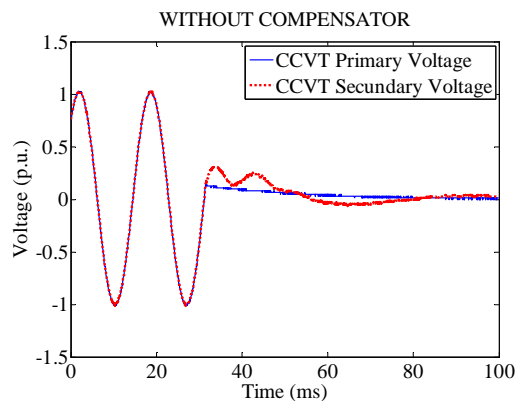

Fig. 13. Operation of the CCVT without the compensator: fault occurrence.
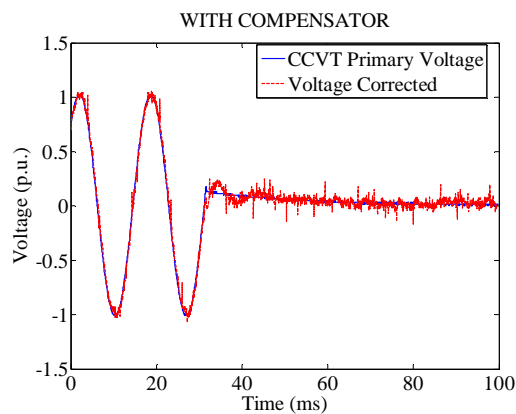

Fig. 14. Operation of the CCVT with the compensator: fault occurrence.

V. CONCLUSIONS

In this paper, a compensator device capable of performing the correction of the CCVT model secondary voltage in real time, was presented. The compensator was designed from the linear parameters of the CCVT and from the ideal frequency response of the compensated CCVT, for a frequency range from 10 Hz to 10 kHz.

Two time domain studies were carried out to evaluate the voltage at the secondary side of a 230 kV CCVT when a disturbance occurred at its primary side: a harmonic source applied to the CCVT primary side; a fault at the CCVT primary side. In both cases, the compensator acted to bring the secondary voltage waveform close to the primary voltage signal.

With the strategy used, the coefficients of the compensator do not depend on the load connected to the CCVT secondary side terminal.

Transient response problems for CCVTs are worst when the ratio of the source impedance over the total line impedance of the line protected is high. In that case, overvoltages may appear at the CCVT primary side. Investigation on that matter is under way to include corrections for the SDT saturation effects in the compensator algorithm.

VII. REFERENCES

[1] Kasztenny, B., Sharples, D., Asaro, V., Pozzuoli, M., "Distance Relays and Capacitive Voltage Transformers-Balancing Speed and Transient Overreach". In: *Annual Conference for Protective Relay Enginners.* College Station Texas, v. 53, 2000.

[2] Pajuelo, E. "An Improved Least Square Voltage Phasor Estimation Technique to Minimize the Impact of CCVT Transients in Protective Relaying". M. Sc. Thesis — University of Saskatchewan Saskatoon - Canada, August 2006.

[3] M. Kezunovic, Lj. Kojovic, V. Skendzic, C. W. Fromen, D. R. Sevcik and S. L. Nilsson, "Digital Models of Coupling Capacitor Voltage Transformers for Protective Relay Transient Studies", *IEEE Trans. on Power Delivery*, vol. 7, pp. 1927-1935, Oct. 1992.

[4] Lj. Kojovic, M. Kezunovic, V. Skendzic, C. W. Fromen and D. R. Sevcik, "A New Method for the CCVT Performance Analysis Using Field Measurements, Signal Processing and EMTP Modeling", *IEEE Trans. on Power Delivery*, vol. 9, pp. 1907-1915, Oct. 1994.

[5] D. A. Tziouvaras, P. McLaren, G. Alexander, D. Dawson, J. Ezstergalyos, C. Fromen, M. Glinkowski, I. Hasenwinkle, M. Kezunovic, Lj. Kojovic, B. Kotheimer, R. Kuffel, J. Nordstrom, S. Zocholl, "Mathematical Models for Current, Voltage and Coupling Capacitor Voltage Transformers", *IEEE Trans. on Power Delivery*, vol. 15, no. 1, pp. 62-72, 2000.

[6] D. Fernandes Jr., "Coupling Capacitor Voltage Transformers Model for Electromagnetic Transient Studies", (in Portuguese), Ph.D. Dissertation, Department of Electrical Engineering, Federal University of Campina Grande, Campina Grande, Brazil, 2003.

[7] E. P. Machado, C. A. Silva, D. Fernandes Jr., W. L. A. Neves, G. R. S. Lira and M. V. Godoy, "A Methodology for Computation of Coupling Capacitor Voltage Transformer Parameters" (in Portuguese), *2008 Brazilian Symposium of Electrical Systems*, Belo Horizonte, Brazil, 2008.

[8] Oppenheim, A. V.; Schafer, R.W. *Discrete-Time Signal Processing*. [S.l.]: Prentice Hall, 1989.

[9] RTDS™ User's Manual Set. RTDS Technologies Inc., pp 3.13, 2007.

VIII. BIOGRAPHY

Célio A. Silva received the B.Sc. and M.Sc. degrees in electrical engineering from Federal University of Campina Grande (UFCG) in 2008 and 2010, respectively. He is currently a Ph.D. student at UFCG. He is with Federal Institute of Education, Science and Technology of Paraíba (IFPB). His research interest is electromagnetic transients in power systems.

Damásio Fernandes Jr. (M'05) received the B.Sc. and M.Sc. degrees in electrical engineering from Federal University of Paraíba, Brazil, in 1997 and 1999, respectively, and the Ph.D. degree in electrical engineering from Federal University of Campina Grande, Brazil, in 2004. Since 2003, he is with the Department of Electrical Engineering of Federal University of Campina Grande. His research interests are electromagnetic transients and optimization methods for power system applications.

Washington L. A. Neves (M'95) is an Associate Professor in the Department of Electrical Engineering at UFCG, Campina Grande, Brazil. He received the B.Sc. and M.Sc. degrees in electrical engineering from UFPB, Brazil, in 1979 and 1982, respectively, and the Ph.D. degree from UBC, Vancouver, Canada, in 1995. From 1982 to 1985 he was with FEJ, Joinville, Brazil. He was a Visiting Researcher with the University of Alberta, Edmonton, Canada, from September 2004 to August 2005, and with UBC, Vancouver, Canada, from September to December 2005. His research interests are electromagnetic transients in power systems and power quality.